Supplementary information for:

Hybrid electrons in the trimerized GaV_4O_8.

Cintli Aguilar-Maldonado[1], Olivier Mentré[1], Alexander A. Tsirlin[2], Clemens Ritter[3], Aleksandr Missiul[4], Francois Fauth[4] and Angel M. Arévalo-López[1]*.

[1] Université Lille Nord de France, UMR 8181 CNRS, Unité de Catalyse et de Chimie du Solide (UCCS USTL), F-59655 Villeneuve d'Ascq, France.

[2] Experimental Physics VI, Center for Electronic Correlations and Magnetism, University of Augsburg, 86159 Augsburg, Germany

[3] Institut Laue-Langevin, 71 Avenue des Martyrs, Grenoble Cedex, France.

[4] CELLS-ALBA Synchrotron, 08290 Cerdanyola, Barcelona, Spain

Electronic structure and magnetic interactions.

The uncorrelated electronic structure of GaV_4O_8 is metallic (Fig. S1) and highlights the different nature of the V1 and V2 electrons. While the V2 states form multiple narrow bands arising from the molecular orbitals of the $V2_3$ triangular units, the V1 states are found around 0 and 2 eV and show the t_{2g}-e_g splitting typical of V^{3+} in the octahedral environment.

Disregarding the weak magnetic moment associated with the $V2_3$ molecules, we mapped the bands in the energy range between -0.1 and +0.5 eV onto a tight-binding model containing V1 t_{2g} states only. This way, we assessed magnetic interactions between the V1 spins and included the effect of the $V2_3$ molecular orbitals implicitly. Hopping parameters t_i of the tight-binding model were used to estimate magnetic exchange couplings as $J_i = 4t_i^2/U_{\mathrm{eff}}$, where U_{eff} = 4 eV is the effective on-site Coulomb repulsion, and the contributions of the two lower-lying t_{2g} orbitals are taken together to account for the two unpaired electrons of $V1^{3+}$. This estimate results in two exchange couplings of similar strength, J_1 and J_2, that together form an hcp-network. Note that the J_i values are taken per bond and normalized to S = 1 of V^{3+}.

We have also calculated the correlated electronic structure using DFT+U and stabilized an insulating solution. This method tends to localize all d-electrons and break orbital molecules regardless of their actual stability. But even such an ultimate localization leads to the same features of charge separation as found experimentally. A robust V^{3+} state is seen on the V1 site with the magnetic moment of nearly 2 μ_B, V2_3 shows a V^{4+}-like state with the magnetic moment of about 1 μ_B, whereas V2_1 and V2_2 display intermediate magnetic moments that are similar in size for both atoms. A similar distribution of the magnetic moments is obtained for several types of collinear magnetic order that could be stabilized for the experimental $Cmc2_1$ crystal structure. A representative density of states is shown in Fig. S2. Here, the V2_3 makes a lower contribution below the Fermi level than V1. On the other hand, the contributions of V2_1 and V2_2 below the Fermi level are similar in size, although they show a somewhat different energy distribution.

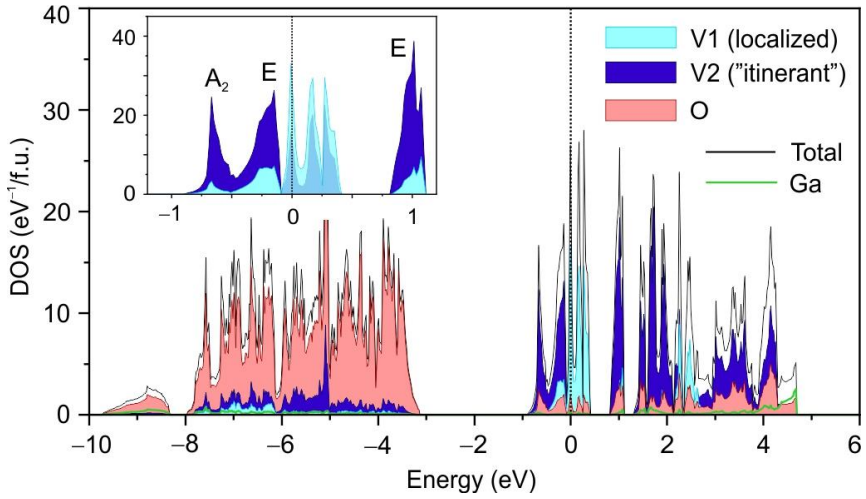

Supp. Fig 1. Uncorrelated electronic structure of GaV_4O_8 showing two distinct types of *d*-electrons: localized electrons of V1 and "itinerant" electrons of V2 that form orbital molecules. The inset displays the peaks of the V2 DOS corresponding to the A_2 and E molecular orbitals of $V2_3$ in Fig. 1d.

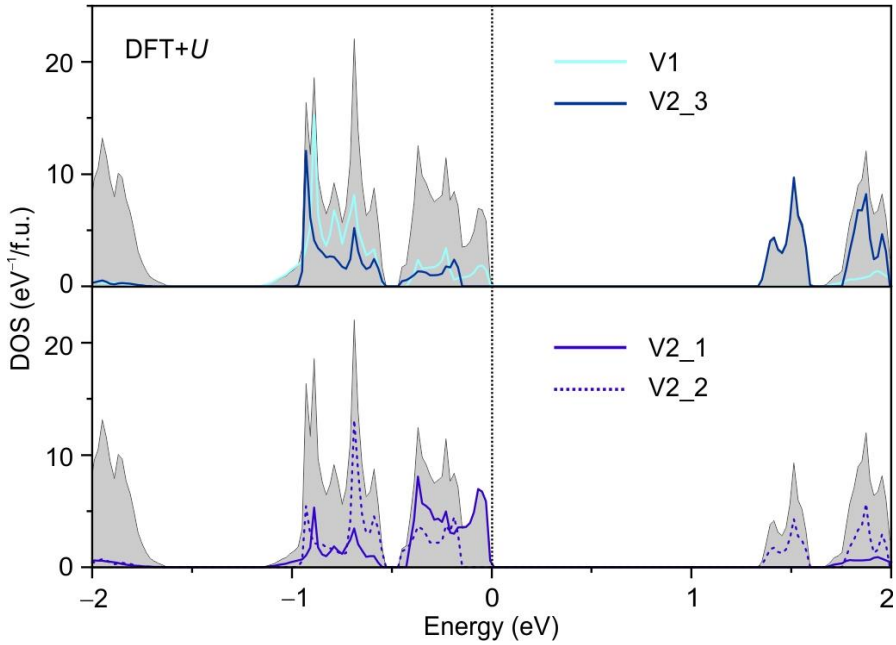

Supp. Fig 2. Electronic structure of GaV_4O_8 calculated on the DFT+*U* level for the sample collinear magnetic structure with the V1 and V2_1 spins aligned parallel to each other and antiparallel to the V2_2 and V2_3 spins, respectively. Both panels show the total DOS (shaded area) as well as atomic-resolved DOS for the majority-spin direction of the respective atom. Note the difference in the number of filled states for V1 vs. V2_3 having different valence (upper panel) and the similarity for V2_1 and V2_2 with the similar valence (lower panel).

Physical properties characterisation.

The temperature dependence of the magnetic susceptibility of GaV_4O_8 is well described by the Curie-Weiss law above 100 K as shown by the inverse susceptibility fit in Supp. Figure 3a. The Weiss temperature of θ = - 28 K indicates antiferromagnetic interactions between the unpaired spins of the vanadium atoms. The Curie constant of C = 1.192 emu K $Oe^{-1}mol\ fu^{-1}$ (μ_{eff} = 1.54 μ_B per V) is significantly reduced from the ideal 3.375 value for 3 x S = 1 and 1 x S = ½ free moments for GaV_4O_8. However, this value approximates to 1.375 for a S = 1 (from $V1^{3+}$) and S = ½ (delocalized in the $V2_3$ trimer) obtained from the unpaired spins.

A kink in the magnetic susceptibility occurs around T_S = 68 K, and a well-defined maximum appears at T_N = 35 K. Magnetisation versus field measurements at 2 K proves an antiferromagnetic transition with M_{9T} = 0.05 μ_B/V (Supp. Fig S3b).

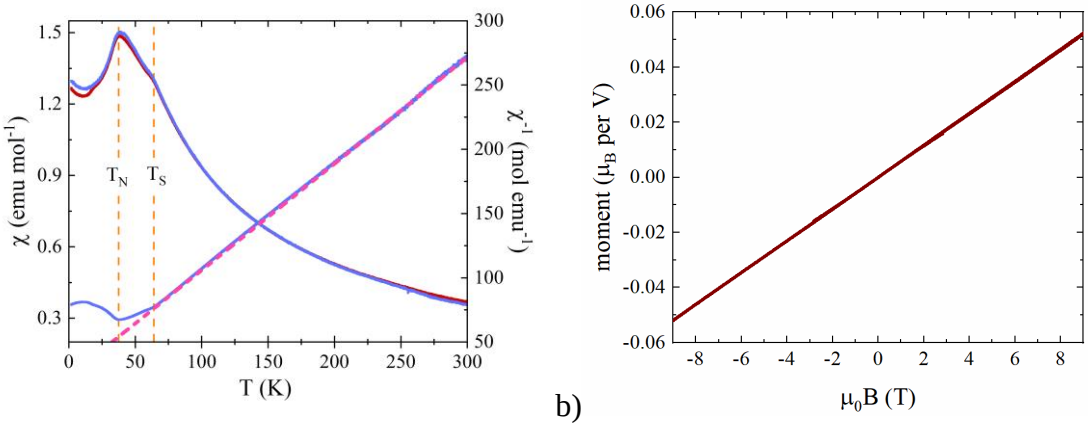

a) b)

Supp. Fig. 3. a) Direct and inverse magnetic susceptibility curves. Vertical broken lines mark the structural transition at T_S = 68 K and the antiferromagnetic transition at T_N = 35 K. Dashed broken line represents the Curie-Weiss fit as discussed above. b) Magnetisation-field loop at 2 K showing a clear AFM signal.

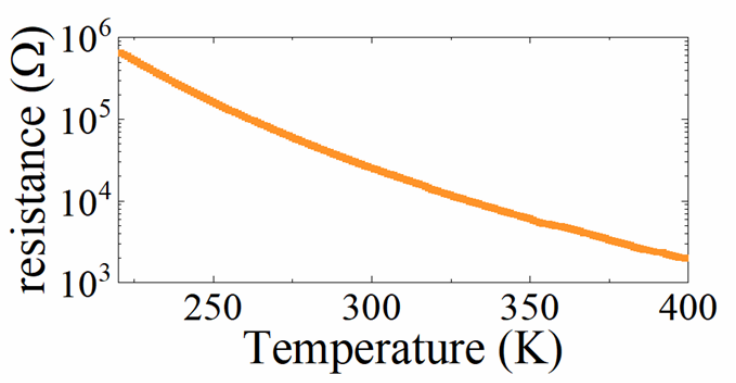

a)

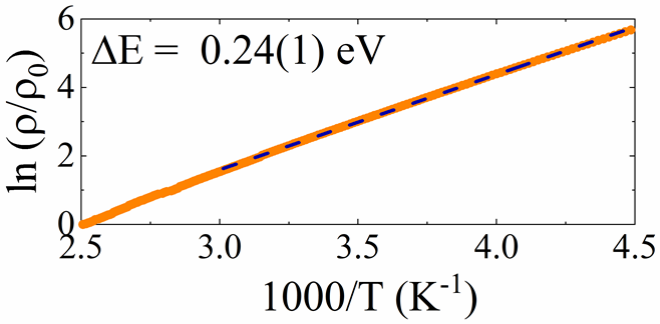

b)

Supp. Fig 4. a) Thermal behaviour of the resistance for GaV_4O_8. Below 220 K the sample is too resistive to measure on our equipment. Arrhenius plot of the electronic resistivity with a ΔE = 0.24(1) eV activation energy.

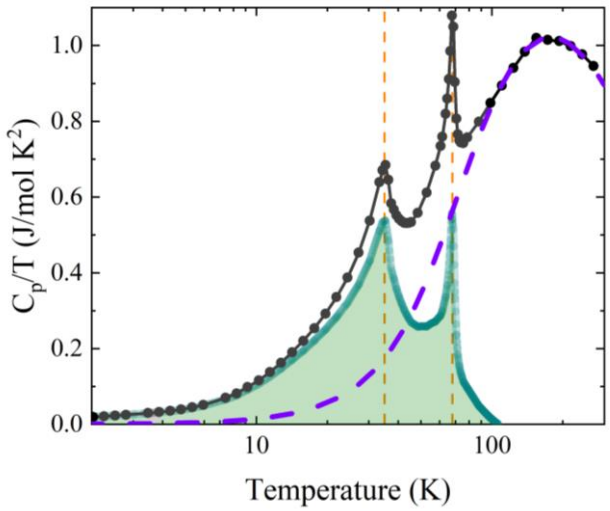

Supp. Fig 5. Heat capacity measurements for GaV_4O_8. The phonon contribution was fitted with a two terms Debye model and a negligible electronic contribution (dashed purple line). Two sharp transitions can be observed at T_S and T_N. Green area corresponds to the heat capacity after removal of the phonon contribution. Applied magnetic fields of up to $\mu_0 H$ = 9 T indicate no effect in the observed maxima, thus confirming the robust AFM nature of the spin ordering below T_N.

Neutron diffraction.

Neutron diffraction was collected at D1B and D20 at the Institute Laue-Langevin, Grenoble, France. Long scans were required at D20 in order to fully resolve the magnetic diffraction as shown in Supp. Fig. 6.

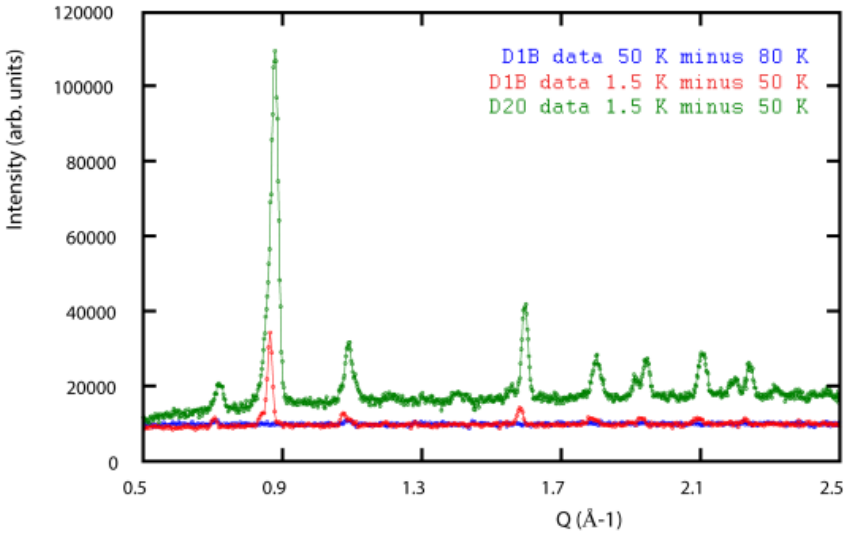

Supp. Fig. 6. Magnetic diffraction obtained from D1B and D20 experiments.

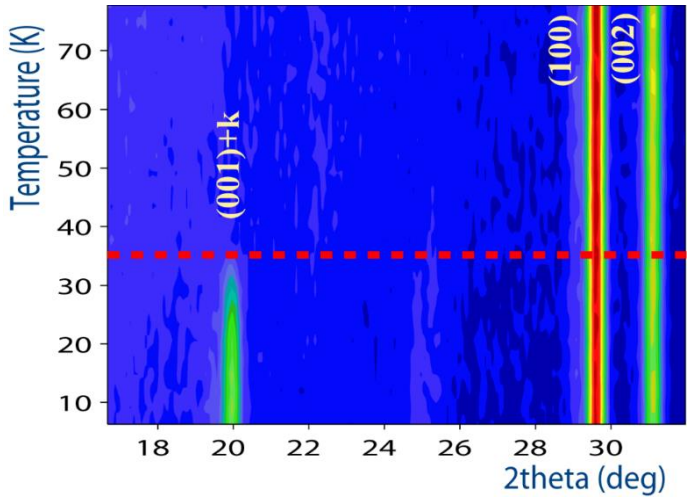

Supp. Fig. 7. D1B neutron powder thermodiffractogram where a clear magnetic intensity can be observed below T_N.

A small contribution from the V_3O_5 secondary phase (<4wt%) was also observed and considered in the analysis.

Figure 3a from the main text shows the best fit to the 1.5 – 50 K difference data from D20 long scans. Attempts to constrain all three V2 moments, or to place a single magnetic moment in the centre of the $V2_3$ triangle by analogy to GaV_4S_8 or $LiZnMo_3O_8$ were unsuccessful.

The local moment values are well scaled by the BVS from Figure 2. They indicate charge order that can be ultimately seen as covalently bonded V^{3+} at the V2_1 and V2_2 sites (higher moment) and V^{4+} at the V2_3 site (lower moment) (Fig. 3c). Besides BVS, this charge distribution is consistent with the magnetic moments from DFT (1.78 μ_B for V1, 1.3-1.5 μ_B for V2_1-V2_2 and 0.99 μ_B for V2_3) and can explain qualitatively the nature of magnetic order in the *ab* plane. Empty orbitals favour ferromagnetic direct- (intra-trimer) or super- (inter-trimer) exchanges between adjacent sites in a V^{4+}-V^{3+}-V^{4+} zig-zag short-long ferromagnetic chains as shown by red (↑) and blue (↓) stripes on Figure 3d, in accordance with Goodenough-Kanamori-Anderson exchange rules or the Kugel-Khomskii orbital scheme. The AFM couplings around the remaining V2 spins in between the stripes are frustrated and minimized by a perpendicular alignment to the other spins.

Synchrotron diffraction.

GaV_4O_8 was measured at ALBA Synchrotron in Barcelona, Spain at the BL04-MSPD beamline with a λ = 0.413 Å wavelength and in a 3 mm capillary and cooled down with a Dyanflow liquid He cryostat (a spurious reflection is seen and marked with an asterisk below). SXRD refinements at low temperatures were done with a mode approach, only values larger than 3σ were allowed to vary.

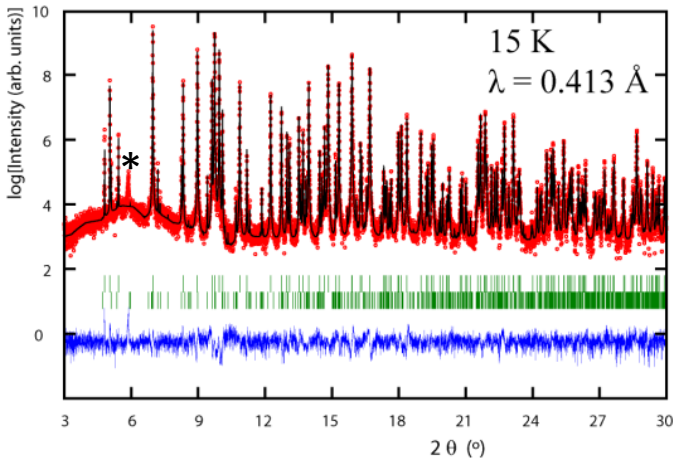

Supp. Fig. 8. SXRD Rietveld refinement for GaV_4O_8 at 15 K. The asterisk refers to diffraction from the diffractometer.

Small single crystals were obtained via chemical vapour transport deposition. A small Ga doping in the V1 site was observed, possibly helping on the crystal growth.

Supp. Table 1. Crystal data and structure refinement.

Crystal data	
Chemical formula	$Ga_{1.069}V_{3.931}O_8$
M_r	402.8
Crystal system, space group	Hexagonal, $P6_3mc$
Temperature (K)	296
a, c (Å)	5.696(4), 9.387(4)
V (Å^3)	263.8 (3)
Z	2
Radiation type	Ag $K\alpha$, λ = 0.56086 Å
μ (mm^{-1})	6.253
Crystal size (mm)	0.05 × 0.05 × 0.05
Data collection	
Diffractometer	Apex
Absorption correction	Multi-scan "SADABS (Bruker, 2000)"
T_{min}, T_{max}	0.6744, 0.7450
No. of measured, independent and observed [$I > 3\sigma(I)$] reflections	2477, 199, 186
R_{int}	0.087
Refinement	
$R[F^2 > 2\sigma(F^2)]$, $wR(F^2)$, S	0.024, 0.048, 1.18
No. of reflections	361
No. of parameters	24
$\Delta\rho_{max}$, $\Delta\rho_{min}$ (e Å^{-3})	0.83, −0.95
Absolute structure	168 of Friedel pairs used in the refinement
Absolute structure parameter	0.05 (5)

Supp. Table 2. Atomic coordinates and equivalent isotropic displacement parameters

Site	x	y	z	Uiso(eq) Å^2	Occupancy
Ga(2b)[a]	1/3	2/3	0.9464	0.0025(3)	1
V1(2b)	1/3	2/3	0.5239(1)	0.0013(5)	0.93(1)/0.07(1)[b]
V2(26c)	0.14833(7)	0.8167(7)	0.2498(1)	0.0026(2)	1
O1(6c)	0	0	0.3818(7)	0.006(1)[c]	1
O2(2a)	1/3	2/3	0.1429(7)	0.004(1)[c]	1
O3(6c)	0.4887(4)	0.5113(4)	0.3794(4)	0.0023(6)[c]	1
O4(6c)	0.1697(4)	0.803(4)	0.6409(5)	0.0045(8)[c]	1

[a] Taken as origin. [b] V/Ga, [c] Refined isotropic

Supp. Table 3. Bond lengths and angles.

$d_{<M-O>}$	(A)	<M-O-M>	(deg)
Ga1-O2	1.845(7)	V2-O1-V2	82.8(3)
Ga1-O3	1.865(4)	Ga1-O2-V2	118.8(2)
V2-O1	1.917(4)	V2-O2-V2	98.7(3)
V2-O2	2.083(3)	Ga1-O3-V1	118.8(2)
V2-O3	2.089(4)	Ga1-O3-V2	118.4(1)
V2-O4	1.882(4)	V1-O3-V2	99.4(1)
V1-O3	2.047(3)	V2-O3-V2	98.4(2)
V1-O4	1.952(3)	V1-O4-V2	136.0(1)
$d_{<M-M>}$	(A)	V2-O4-V2	84.7(2)
V2-V2	3.161(3)		
V1-V1	5.696(5)		
V1-V2	3.154(2)		
Ga-V1	3.368(3)		
Ga-V2	3.398(1)		

Supp. Table 4. Anisotropic displacement parameters

Site	U_11	U_22	U_33	U_12	U_13	U_23
Ga(2b)	0.0024(3)	0.0024(3)	0.0026(5)	0.0012(1)	0	0
V1(2b)	0.0006(6)	0.0006(6)	0.0027(8)	0.0003(3)	0	0
V2(6c)	0.0024(3)	0.0024(3)	0.0027(4)	0.0010(3)	-0.0001(2)	0.0001(2)

Supp. Table 5. Atomic coordinates and selected V-V distances of GaV_4O_8 from the Rietveld fit of 90 K SXRD data. S.G. P6_3mc, a = 5.68436(2) Å, c = 9.38271(4) Å. R_{exp} = 0.099 R_p = 0.113, χ^2 = 1.99.

Site	x	y	z	Biso (Å^2)
Ga(2b)	1/3	2/3	0.0596(9)	0.04(1)[a]
V1(2b)	2/3	1/3	0.1366(9)	0.04(1) [a]
V2(6c)	0.2964(2)	0.1482(1)	-0.1372(8)	0.04(1) [a]
O1(6c)	0.5121(5)	1.024(1)	-0.0066(9)	0.2(4)[b]
O2(6c)	-0.1695(4)	0.1695(4)	0.2528(9)	0.2(4) [b]
O3(2b)	1/3	2/3	0.255(1)	0.2(4) [b]
O4(2a)	0	0	0	0.2(4) [b]
V2-V2	2.527(2) Å	V1-V2	3.15(1) Å	
V2-V2	3.157(2) Å	V1-V2	3.552(7) Å	

[a], [b] constrained together.

Supp. Table 6. Atomic coordinates and selected V-V distances of GaV_4O_8 from the Rietveld fit of 15 K SXRD data. S.G. $Cmc2_1$, a = 5.68256(5) Å, b = 9.8471(1) Å, c = 9.38353(4) Å. R_{exp} = 0.095 R_p = 0.113, χ^2 = 2.07.

Site	x	y	z	Biso (Å^2)
Ga1 (4a)	0	2/3	0.0595	0.06(1)[a]
V1_1(4a)	0	2/3	0.6366	0.06(1)[a]
V2_1(8b)	0.2210(6)	0.0737(2)	0.3595(3)	0.06(1)[a]
V2_3(4a)	0	0.1499(8)	0.8692(6)	0.06(1)[a]
O1_1(8b)	0.76807	0.25603	-0.0067	0.1(5)[b]
O1_2(4a)	0	0.51205	0.4933	0.1(5)[b]
O2_1(8b)	0.254(1)	0.4181(5)	0.250(1)	0.1(5)[b]
O2_2(4a)	0	0.819(2)	0.758(2)	0.1(5)[b]
O3_1(4a)	0	0.678(2)	0.2547	0.1(5)[b]
O4_1(4a)	0	0	0	0.1(5)[b]
V2_1-V2_1	2.512(7) Å	V1_1-V2_1	3.180(3) Å	
V2_1-V2_3	2.536(8) Å	V1_1-V2_3	3.092(7) Å	
V2_1-V2_3	3.151(8) Å	V1_1-V2_1	3.534(3) Å	
		V1_1-V2_3	3.587(4) Å	

[a], [b] constrained together.

Supp. Table S7. GaV_4O_8 magnetic structure refinement from D20 (λ = 2.41 Å) at 1.5 K. Following ISODISTORT from the mΛ2 irrep obtained from *P6₃mc* space group and *k* = [¼ ¼ 0] magnetic propagation vector with only one arm of the star. Pa_c magnetic space group (7.27) with *a* = 11.29037 Å, *b* = 9.81738 Å, *c* = 14.64098 Å and *β* = 140.3866 º ({(2, 2, 0), (-1, 1, 0), (2, 2, 1)} supercell). R_{mag} = 8.87 %.

	x	y	z	m_x	m_y	m_z	m_{Tot} (μ_B)
V1_1	0.6083	0.8333	0.3853	0	-1.06(1)	0	1.06(1)
V1_2	0.8583	0.3333	0.3853	0	-1.06(1)	0	1.06(1)
V2_1a	0.6322	0.1482	0.6322	0	-0.225(7)	0	0.225(7)
V2_1b	0.8822	0.6482	0.6322	0	0.225(7)	0	0.225(7)
V2_2a	0.2434	0.0741	0.1322	0.40(1)	0	0	0.40(1)
V2_2b	0.4934	0.5741	0.1322	0	-0.40(1)	0	0.40(1)
V2_3a	0.5210	0.9259	0.6322	0	-0.40(1)	0	0.40(1)
V2_3b	0.7710	0.4259	0.6322	-0.40(1)	0	0	0.40(1)